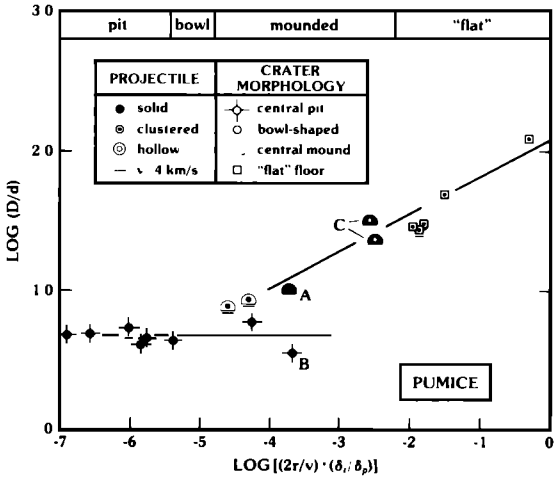

Fig. 12*a*

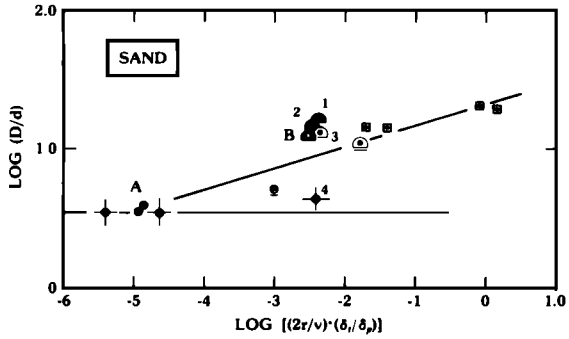

Fig. 12*b*

Fig. 12. The combined effects of target/projectile density (δ_t/δ_p) and time for projectile-target contact on crater aspect ratio and morphology. The projectile-target contact time is given by the projectile diameter $2r$ divided by the impact velocity v. Figure 12*a* shows that both crater morphology and aspect ratio for clustered and weak impactors systematically vary with the contact time and target-projectile density ratio. Competent, single-body impactors, however, are uncorrelated with these parameters and form pitted crater floors. The least squares fit applies only to clustered impactors represented by open symbols: $\log D/d = 0.267 \log [(2r/v) \cdot (\delta_t/\delta_p)] + 2.072$ (correlation coefficient of 0.981). Lettered symbols are identified in Figure 11*a*. Figure 12*b* also shows good correlation for impacts into sand in contrast with Figure 11*b*. The lettered and numbered data points are identified with Figure 11*b*. The least squares fit (including point B) gives: $\log D/d = 0.148 \log [(2r/v) \cdot (\delta_t/\delta_p)] + 1.318$ (correlation coefficient of 0.849).

referred to the downrange axis becomes smaller) with smaller impact angles. Single-body impacts (Figure 18) produce relatively small zones of avoidance uprange, thereby suggesting that cluster dispersion also may control the ejecta patterns. Figure 19 explicitly demonstrates this fact and shows a systematic change in the zone of ejecta avoidance uprange, the apex angle of the principal herringbone pattern, and the apex angle of the downrange ejecta fan zone.

Oberbeck and Morrision [1974] produced herringbone patterns experimentally by two adjacent simultaneous impacts and demonstrated how such patterns result from the simple interaction of the two expanding, cone-shaped ejecta curtains. The results presented here indicate that the herringbone pattern can also be produced by much more complicated interactions of hundreds to thousands of small impactors. Four other significant differences between clustered and double impacts can be cited that might prove useful as diagnostic clues for clustered impacts on planetary surfaces. First, simultaneous double impacts produce herringbone ridges with apex angles much larger than those for clustered impacts at the same impact angle. Second, herringbone ridges wrap around the uprange rim at modest impact angle (45°), whereas two-body impacts do not develop such a pattern to the same degree. Third, many herringbone ridges can develop around the same crater for clustered impacts, whereas two-body impacts are dominated by a single septum dividing each crater. Fourth, the herringbone ridges bend downrange in clustered impacts at 45° (see Figure 17*b*). Although two-body impacts also produce this downrange bending of the herringbone pattern, the inflection is restricted to the distal ends of the ejecta.

The clustered impacts produced by shattered pyrex spheres form a relatively well-defined cloud of projectiles. This may not be the configuration for either primary or secondary impacts on planetary surfaces. Consequently, an experiment was performed with the rupturing diaphragm oriented obliquely to the flight direction. Figure 20 shows that the resulting crater resembles those craters previously described except that the axis of syymmetry does not parallel the impact direction. *Oberbeck and Morrison* [1974] found the same type of offset for two-body impacts.

5. Ejecta Dynamics and Distribution of Postimpact Projectile Materials

The evolution of the ejecta plume for clustered impacts is significantly different from plume evolution for single-body impacts. In this section we compare such differences for vertical and oblique impacts at velocities from 1.3 to 1.8 km/s. A more detailed discussion of ejecta dynamics with comparisons at higher impact velocities (6 km/s) will be considered in a separate paper. A preliminary account, however, can be seen in the work by *Schultz and Gault* [1983]. The qualitative examination here is intended to place the preceding descriptions in the context of the cratering process. Also in this section, we examine the distribution of projectile material resulting from a clustered impact. Such considerations have important implications for understanding the lateral transport of primary ejecta, the mixing process, and the spectral signature of primary material following a low-velocity secondary impact.

5.1. *Ejecta Dynamics*

For any given dispersion, vertical impact by clustered projectiles consistently produces a very distinctive sequence of plume growth. Figure 21 permits comparison of such a sequence (Figure 21*b*) with a single-body impact having about the same mass and velocity (Figure 21*a*). The entire cloud of projectiles impacts well within one frame of the high-speed sequence, i.e., the interframe time interval of 0.1 ms, and an expanding amorphous cloud is quickly formed. This cloud eventually forms a well-defined boundary inclined at a low angle (<15°) from the surface. This ejecta curtain gradually